Self-consistent electron-mobility calculation in a modulation-doped two-dimensional electron gas

Vincenzo Piazza
Scuola Normale Superiore and Istituto Nazionale di Fisica della Materia, I-56100 Pisa, Italy

Paolo Casarini
Istituto di Fisica dell'Università di Modena and Istituto Nazionale di Fisica della Materia, I-41100 Modena, Italy

Silvano De Franceschi, Marco Lazzarino, and Fabio Beltram
Scuola Normale Superiore and Istituto Nazionale di Fisica della Materia, I-56100 Pisa, Italy

Carlo Jacoboni
Istituto di Fisica dell'Università di Modena and Istituto Nazionale di Fisica della Materia, I-41100 Modena, Italy

Antonio Bosacchi and Secondo Franchi
Istituto MASPEC del Consiglio Nazionale delle Ricerche, I-43100 Parma, Italy
(Received 25 November 1997)

We present a fully self-consistent model to calculate the low-temperature mobility of a modulation-doped two-dimensional electron gas. Ionized impurity scattering and level broadening are included, yielding a parameter-free quantitative determination of the electron mobility. Our theoretical results are verified experimentally by Hall-effect measurements performed on an *n*-type modulation-doped GaAs/$Al_xGa_{1-x}As$ single-quantum-well heterostructure. [S0163-1829(98)02615-0]

Modern epitaxial growth techniques have had a dramatic effect on semiconductor physics. In fact it is now possible to tailor the band diagram of heterostructures with great freedom and achieve by *material design* a large variety of electronic states and properties.[1]

Accurate design of these structures can often be obtained by self-consistent Schrödinger-Poisson solvers easily implemented within the effective mass framework.[2] There is, however, another important property that can be *designed* in semiconductor heterostructures thanks to the concept of modulation doping.[3] By appropriate choice of the spatial separation between free carriers and doping layers it is possible to tune not only the free carrier density, but also its mobility. This scheme opened the way to the exploration of new physical phenomena (e.g., the quantum Hall effect[4]) and to the implementation of device concepts (e.g., the *modulation-doped field-effect transistor*[5]). In this paper we present and verify experimentally a fully self-consistent method to calculate the low-temperature mobility of a modulation-doped two-dimensional electron gas in the general case of multisubband occupation, including the effect of ionized impurity scattering and level broadening. This scheme allows the precise calculation of static and dynamic electronic properties for the accurate design of heterostructure composition.

From the theoretical point of view, transport properties of a quantum well (QW) in the general case of many occupied electronic subbands can be described by a system of coupled Boltzmann equations. To solve these equations it is necessary to know the relaxation times $\tau_i(\varepsilon)$ for each occupied subband i. The $\tau_i(\varepsilon)$'s, at zero temperature, are given by[6,7]

$$\tau_i(\varepsilon)=\sum_j K_{ij}^{-1}(\varepsilon)(\varepsilon-E_j), \tag{1}$$

where E_j is the energy of jth level, and ε is the electron energy. The matrix $K_{ij}(\varepsilon)$ includes all the information about the system and, therefore, depends on the scattering mechanisms included.

In modulation-doped heterostructures at low temperatures, the dominant scattering mechanism is Coulomb interaction between carriers and ionized impurities. We account for this mechanism including the screening effects in the random-phase approximation using realistic eigenstates for the QW obtained by means of a self-consistent Poisson-Schrödinger solver. We underline that composition and dopant concentration profiles are the only information required in our theoretical analysis: no fitting parameters are employed.

The Fermi golden rule leads to an energy-conserving transition probability. With this assumption the matrix $K_{ij}(\varepsilon)$ can be written as[8]

$$K_{ij}(\varepsilon)=\frac{\hbar^3}{8\pi^2 m^2}\int d\boldsymbol{k}\int d\boldsymbol{k}'\Bigg[\sum_l k^2\delta_{ij}\delta(\varepsilon-\varepsilon_i(k))\times W_{il}(\boldsymbol{k}-\boldsymbol{k}')\,\delta(\varepsilon-\varepsilon_l(k'))-\boldsymbol{k}\cdot\boldsymbol{k}'\,\delta(\varepsilon-\varepsilon_j(k'))\times W_{ij}(\boldsymbol{k}-\boldsymbol{k}')\,\delta(\varepsilon-\varepsilon_i(k))\Bigg], \tag{2}$$

where m is the electronic effective mass, $\varepsilon_i(k)=E_i+(\hbar^2k^2/2m)$. $W_{ij}(\boldsymbol{k}-\boldsymbol{k}')$ is the squared matrix element of the perturbation from state $i\boldsymbol{k}$ to state $j\boldsymbol{k}'$ averaged over the ionized impurity distribution $N_D^+(\boldsymbol{R})$:

$$W_{ij}(\boldsymbol{k}-\boldsymbol{k}') = \int d^3\boldsymbol{R} N_D^+(\boldsymbol{R}) \times \left| \sum_{i'j'} \epsilon^{-1}_{i'j'ij}(\boldsymbol{k}-\boldsymbol{k}') \langle j\boldsymbol{k}'|V(\boldsymbol{r}-\boldsymbol{R})|i\boldsymbol{k}\rangle \right|^2, \tag{3}$$

where $V(\boldsymbol{r}-\boldsymbol{R})$ is the potential, calculated in $\boldsymbol{r}$, due to an ionized impurity located at $\boldsymbol{R}$, and $\epsilon^{-1}_{i'j'ij}(\boldsymbol{q})$ is an effective dielectric constant that accounts for screening[7] including the effect of virtual excitation to unoccupied subbands. Equation (2) contains all the information needed to calculate electronic transport properties: electronic wave functions, the ionized impurity distribution (both entering the definition of W_{ij}) and Fermi energy.

Energy-level broadening plays an important role in determining the electron mobility. This is particularly important here since, owing to the electrostatic nature of Coulomb interaction, the scattering probability increases by decreasing Fermi energy. The broadening of the states for the first-excited subband therefore increases when the subband population decreases. This can be rigorously treated in the quantum transport framework.[9] Unfortunately, the rather cumbersome algebra involved limits the applicability of this formalism to very simple systems only.

Here we include level-brodening effects in the Boltzmann transport equation by replacing in the Fermi golden rule the energy-conserving δ functions by Lorentzian functions. Their widths Γ_j are calculated by means of Green-function techniques, as shown in Ref. 9, and using the same effective potential V_{ij}^{eff} as above. Thus no phenomenological parameters are required.

The resulting $K_{ij}(\varepsilon)$ matrix is

$$K_{ij}(\varepsilon) = \frac{\hbar^3}{8\pi^2 m^2} \int d\boldsymbol{k} \int d\boldsymbol{k}' \Big\{ \sum_l k^2 \delta_{ij} \delta(\varepsilon-\varepsilon_i(k)) \times [W_{il}(\boldsymbol{k}-\boldsymbol{k}')\Delta_{il}(k,k')\theta(\varepsilon_l(k')-\varepsilon) + W_{li}(\boldsymbol{k}'-\boldsymbol{k}) \times \Delta_{li}(k',k)\theta(\varepsilon-\varepsilon_l(k'))] - \boldsymbol{k}\cdot\boldsymbol{k}'\,\delta(\varepsilon-\varepsilon_j(k')) \times [W_{ji}(\boldsymbol{k}'-\boldsymbol{k})\Delta_{ji}(k',k)\theta(\varepsilon_i(k)-\varepsilon) + W_{ij}(\boldsymbol{k} - \boldsymbol{k}')\Delta_{ij}(k,k')\theta(\varepsilon-\varepsilon_i(k))] \Big\}, \tag{4}$$

where

$$\Delta_{ij}(k,k') = \frac{1}{\pi} \frac{\Gamma_j(k')}{[\varepsilon_i(k)-\varepsilon_j(k')]^2 + \Gamma_j^2(k')} \tag{5}$$

and $\theta(x)$ is the Heavyside step function.

In order to test our model we have studied the transport properties of a gated n-type modulation-doped $Al_{0.25}Ga_{0.75}As$/GaAs QW heterostructure, whose composition is shown in Table I. By appropriately biasing the gate it was possible to explore transport in both single- and double-subband occupation regimes.

The heterostructure was grown by molecular-beam epitaxy at 600 °C, with As_4/(Al+Ga) and As_4/Ga beam equivalent pressure ratios of 12.5 and 15.5 and with GaAs and $Al_xGa_{1-x}As$ growth rates of 1.0 μm h^{-1} and 0.75 μm h^{-1}.

TABLE I. Nominal composition of the structure.

Material	Thickness (nm)	Doping (cm^{-3})
GaAs	5	undoped
$Al_{0.25}Ga_{0.75}As$	27	undoped
$Al_{0.25}Ga_{0.75}As$	27	n 7×10^{17}
$Al_{0.25}Ga_{0.75}As$	10	undoped
GaAs	20	undoped
$Al_{0.25}Ga_{0.75}As$	10	undoped
$Al_{0.25}Ga_{0.75}As$	11	n 7×10^{17}
$Al_{0.25}Ga_{0.75}As$	40	undoped
GaAs	500	undoped

[a]Semi-insulating GaAs substrate.

Hall-bar mesas were patterned by standard photolithographic techniques and wet-chemical etching. Au/Ge Ohmic contacts were alloyed for transport measurements; a Schottky gate was evaporated on the channel surface covering ~65% of its area.

The need for high carrier concentration lead to the choice of very narrow spacer layers (100 Å) in our structure. Consequently the results of the simulations are very sensitive to the doping profile. The latter was verified by SIMS and C-V measurements showing significant segregation (~10 nm) and diffusion of dopant (Si) impurities, consistently with the results reported by Pfeiffer *et al.*[10] The full width at half-maximum and average concentration of the doping layer grown before (after) the QW were ~14 nm (~31 nm) and ~7.9×10^{17} atoms/cm^3 (~7.3×10^{17} atoms/cm^3), respectively.

The charge density in the QW was determined by Shubnikov–de Haas measurements. Figure 1(a) shows the data obtained at 1.2 K and zero gate bias: two oscillations of

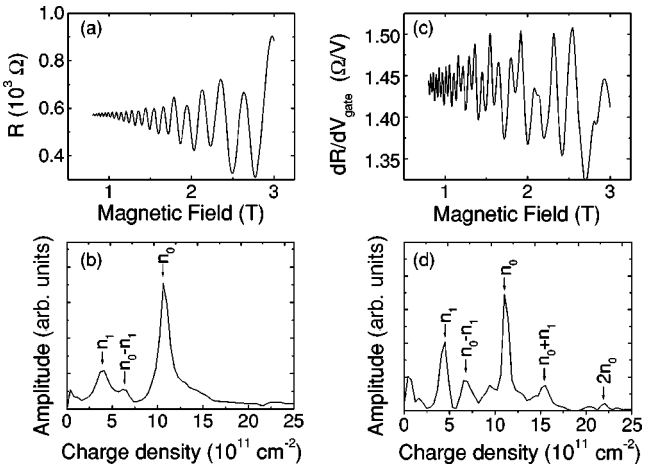

FIG. 1. Magnetoresistance oscillations [(a) and (c)] and their Fourier analysis [(b) and (d)] obtained at 1.2 K and zero gate bias from the sample of Table I. (c) is taken with the phase-sensitive technique described in the text; its FT (d) shows clearly two peaks due to two populated subbands, one with a carrier density of $\approx11\times10^{11}$ cm^{-2}, the other with a carrier density of $\approx4\times10^{11}$ cm^{-2}. (a) was obtained by the standard dc technique: note that the onset of the oscillations occurs at higher magnetic fields with respect to (c) and the signal due to the second subband is less visible.

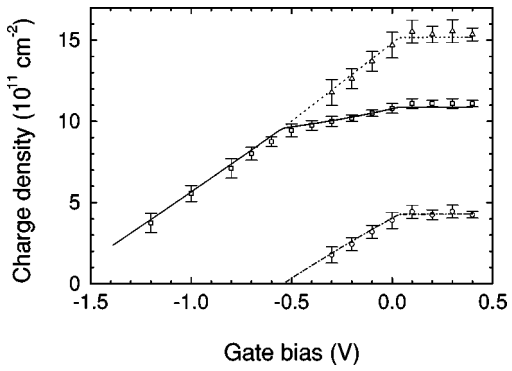

FIG. 2. Carrier concentration in the QW *versus* gate bias at 4.2 K. Circles, measured second subband population; squares, first subband population; triangles, total concentration. Dash-dotted line, calculated second subband population; solid line, first subband population; dotted line, total concentration.

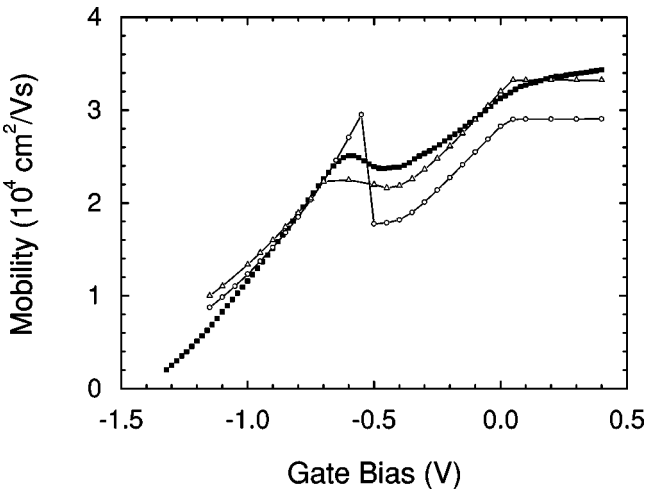

FIG. 3. Mobility of carriers *versus* gate bias at 4.2 K. Solid squares: Hall mobility. Open triangles: calculated mobility including level broadening. Open circles: calculated mobility without level broadening.

different period are visible, confirming that two subbands are populated; Fourier transform (FT) analysis of the data [Fig. 1(b)] gives the carrier density in each subband (n_0 for the ground subband, n_1 for the first excited one).

To determine the value of the gate bias ($V_{\rm tr}$) corresponding to the transition from two to one occupied subbands we measured the charge density as a function of $V_{\rm gate}$. The oscillations due to the second subband, though visible at $V_{\rm gate}=0$ V, are progressively depressed as the channel is depleted; thus, the determination of $V_{\rm tr}$ is not straightforward. This problem was solved using a technique somewhat analogous to that proposed by Schacham, Haugland, and Alterovitz,[11] which consists in measuring the derivative of the magnetoresistance with respect to the charge density. This technique enhances the oscillations at lower magnetic fields and, in particular, those due to the scarcely populated subbands, allowing the measurement of very low electron densities. Differentiation with respect to the density was achieved by adding a small ac voltage to the gate bias (15 mV) and monitoring the voltage drop across the channel by a lock-in amplifier.

Figure 1(c) shows the data taken in the same experimental conditions of those reported in Fig. 1(a), but with the phase-sensitive technique. FT of these data is reported in Fig. 1(d); the amplitudes of the peaks associated with the two subbands have now comparable magnitude; in particular, the peak labeled n_1 is sharper than the corresponding one in Fig. 1(b). Some other peaks appear at n_0-n_1 and n_0+n_1. They are due to the intermodulation of the two-subband oscillations and are related to intersubband scattering.[12,13]

Carrier concentration as a function of gate bias is shown in Fig. 2: above -0.3 V two peaks are clearly visible, corresponding to two subbands being populated; below -0.6 V single-subband occupation is unambiguously observed. By extrapolating the linear fit to n_1, for gate biases between -0.3 V and 0 V, we estimated $V_{\rm tr}=-0.54\pm0.07$ V. The solid lines in Fig. 2 are obtained by solving self-consistently the Poisson and Schrödinger equations for our structure including the experimentally determined doping profile.

The mobility of the sample was obtained by Hall measurements at 4.2 K (solid squares in Fig. 3). Experimental data show a marked drop at gate biases near $V_{\rm tr}$. This corresponds to the onset of intersubband scattering.[7,14]

The wave functions and the electronic subbands obtained by the Poisson-Schrödinger solver at different gate biases were used to calculate the mobility of the sample, according to the model described above. The comparison between the experiment and the calculations is reported in Fig. 3 showing excellent agreement when level broadening is included. The residual discrepancy at lower gate biases is linked to multiple scattering events[15] which are not taken into account in our calculations.

In summary, we have presented a model to calculate the multichannel transport properties of a semiconductor heterostructure, which includes level broadening self-consistently, with no phenomenological parameters. The results of our model were compared to the experimental data obtained from a single $Al_{0.25}Ga_{0.75}As/GaAs$ modulation-doped QW heterostructure by Hall measurements showing excellent agreement.

[1] F. Capasso, J. Vac. Sci. Technol. B **1**, 457 (1983); F. Capasso, Science **235**, 172 (1987).

[2] G. Bastard, *Wave Mechanics Applied to Semiconductor Heterostructures* (Les éditions de physique, Paris, France, 1988) Chap. 5.

[3] R. Dingle, H. L. Stormer, A. C. Gossard, W. Wiegmann, Appl. Phys. Lett. **33**, 665 (1978).

[4] K. von Klitzing, G. Dorda, and M. Pepper, Phys. Rev. Lett. **45**, 494 (1980).

[5] S. Wang, *Fundamentals of Semiconductor Theory and Device Physics* (Prentice-Hall, Englewood Cliffs, NJ, 1989).

[6] E. D. Siggia and P. C. Kwok, Phys. Rev. B **2**, 1024 (1970).

[7] S. Mori and T. Ando, J. Phys. Soc. Jpn. **48**, 865 (1980).

[8] S. Mori and T. Ando, Phys Rev. B **19**, 6433 (1979).

[9] D. G. Cantrell and P. N. Butcher, J. Phys. C **18**, 5111 (1985).
[10] L. Pfeiffer, E. F. Schubert, and K. W. West, Appl. Phys. Lett. **58**, 2258 (1991).
[11] S. E. Schacham, E. J. Haugland, and S. A. Alterovitz, Appl. Phys. Lett. **61**, 551 (1992).
[12] P. T. Coleridge, Semicond. Sci. Technol. **5**, 961 (1990).
[13] J. Herfort and Y. Hirayama, Appl. Phys. Lett. **69**, 3360 (1996).
[14] H. L. Stormer, A. C. Gossard, and W. Wiegmann, Solid State Commun. **41**, 707 (1982).
[15] A. Gold, Appl. Phys. Lett. **54**, 2100 (1989).